CHAPTER 18

Sarcoidosis: imaging features

J.A. Verschakelen

Dept of Radiology, University Hospitals, Leuven, Belgium.

Correspondence: J. Verschakelen, Dept of Radiology, University Hospitals, Herestraat 49, B-3000 Leuven, Belgium. Fax: 32 16343765; E-mail: johny.verschakelen@uz.kuleuven.ac.be

Sarcoidosis is a granulomatous disease of unknown aetiology that shows multisystemic involvement and that is predominantly seen in young and middle-aged patients, with a slightly higher prevalence in females [1]. The histological hallmark of sarcoidosis is noncaseating granulomas with proliferation of epitheloid cells [2]. Although the disorder is multisystemic, pulmonary manifestations typically dominate. Chest radiographs are abnormal in 90–95% of patients with bilateral hilar adenopathy as the most common radiological finding [1, 3]. Although cough and dyspnoea may be present in patients with thoracic involvement, 30–60% of the patients are asymptomatic making the findings on the chest radiograph incidental. The initial manifestation of the disease can also be related to the involvement of structures outside the chest [1, 3, 4]. Although skin and ocular lesions are most common, the liver, spleen, parotid glands, central nervous system (CNS), genitourinary system, and the bones and muscles may also be involved.

The diagnosis of sarcoidosis is commonly established on the basis of clinical and radiological findings supported by histological findings. Thoracic involvement is often easily recognised on a chest radiograph when hilar adenopathy is present (fig. 1). However, although probably not necessary in every patient, computed tomography (CT) and High-resolution CT (HRCT) can play an important role in the diagnosis and staging

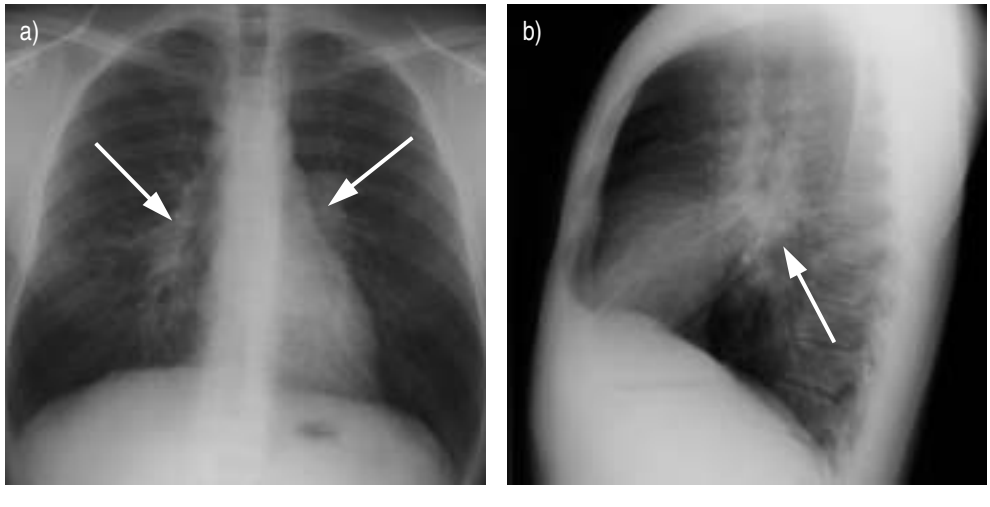

Fig. 1. – a) Posteroanterior and b) lateral chest radiograph show broadening of the paratracheal mediastinum, nodular opacities in both hila (white arrows) and a convex border of the aortic pulmonary window caused by enlarged lymph nodes. Notice also some reticular involvement of the lung parenchyma.

Eur Respir Mon, 2005, 32, 265–283. Printed in UK - all rights reserved. Copyright ERS Journals Ltd 2005; European Respiratory Monograph; ISSN 1025-448x. ISBN 1-904097-22-7.

of thoracic sarcoidosis (fig. 2) [5]. CT cannot only demonstrate subtle mediastinal adenopathy, which is hardly or not visible on a chest radiograph, but can also better show lung parenchymal involvement. Moreover, some (HR)CT features are moderately characteristic for the disease. Although magnetic resonance imaging (MRI) may be useful in the evaluation of mediastinal and pulmonary involvement, the main development of this technique has taken place in the evaluation of neurosarcoidosis, and to a lesser degree in bone, muscle and cardiac sarcoidosis [6].

In this review the radiological presentation of sarcoidosis will be discussed and illustrated. The review will start with a description of the radiograph and CT features of mediastinal and pulmonary involvement of sarcoidosis and the correlation of these features with disease activity and pulmonary function. Also, a paragraph on cardiac involvement is included. In the second part the imaging characteristics of selected extrathoracic manifestations of sarcoidosis will be discussed briefly.

Intrathoracic manifestations of sarcoidosis

Common features

Lymphadenopathy. More than 80% of the patients with sarcoidosis have intrathoracic adenopathy at the time of the presentation [7–9]. These enlarged lymph nodes are classically located in both hila, in the pre- and right paratracheal mediastinum, in the aortopulmonary window, in the subcarinal area and, less frequently, in the anterior and posterior mediastinum. However, only the right paratracheal and hilar lymph nodes and those located in the aortic pulmonary window can easily identified on a posteroanterior and lateral chest radiograph (fig. 1) [10–12]. A CT examination is usually necessary to show the involvement of the other node groups (fig. 2) [12]. Although contrast-enhanced (CE) CT will better differentiate between enlarged lymph nodes and the vascular structures in the mediastinum, and especially in the hila, injection of contrast is not always necessary to make the diagnosis. Mediastinal adenopathy without hilar involvement or with unilateral hilar involvement is rare but can be seen especially in older patients [13]. HAMPER *et al.* [14] found unilateral hilar adenopathy in six out of 29 patients who were aged >50 yrs when the initial diagnosis of sarcoidosis was made. In this study, two patients had isolated mediastinal lymph node enlargement. Calcification can occur in affected nodes, especially in patients with longstanding sarcoidosis, and

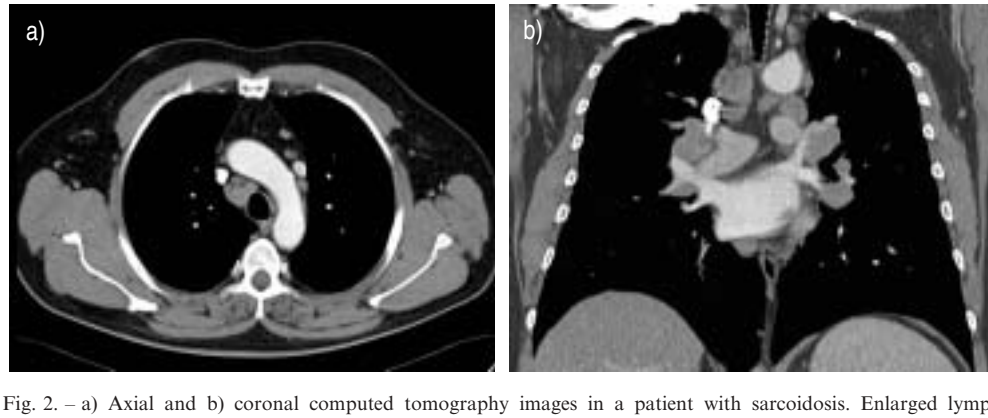

Fig. 2. – a) Axial and b) coronal computed tomography images in a patient with sarcoidosis. Enlarged lymph nodes can be seen in the mediastinum and in both hila.

can be amorphous, punctuate, or eggshell (fig. 3) [7, 13]. One study, examining nodes with CT in 49 patients with biopsy-proven sarcoidosis, showed nodal calcification in 53% of patients [15]. Hilar adenopathy was often bilateral, while the eggshell pattern was seen in 42% of patients with nodal calcification [16, 17].

Pulmonary parenchymal disease. Lung involvement in sarcoidosis is present in 25–50% of patients and has a strong predilection for the upper lung [3, 4]. In addition, although both diffuse and peripheral patterns are seen, the abnormalities are often centrally distributed [18].

Chest radiograph. Reticular, reticulonodular or focal alveolar opacities are the most characteristic features on a chest radiograph (fig. 4a–c) [14, 19]. Confluent areas of lung consolidation and multiple well-circumscribed pulmonary nodules are less commonly seen [14, 20–23]. A ground-glass pattern is only very rarely present [24]. End-stage disease may manifest as conglomerated masses, and broad and coarse septal bands with architectural distortion, hilar retraction, upper lobe volume loss and, finally, honeycomb change and large bullae (fig. 4d). Extensive calcification may be encountered within fibrotic granulomas [13]. These processes are usually seen predominantly in the central and upper lung; a distribution that is typical for sarcoidosis, but can also be seen in tuberculosis and silicosis. In advanced fibrosis, enlarged pulmonary arteries indicating pulmonary arterial hypertension and bronchiectasis may be observed.

Computed tomography. Pulmonary infiltrates and their distribution pattern are usually better appreciated on a CT examination. The cross-sectional format of CT allows a better

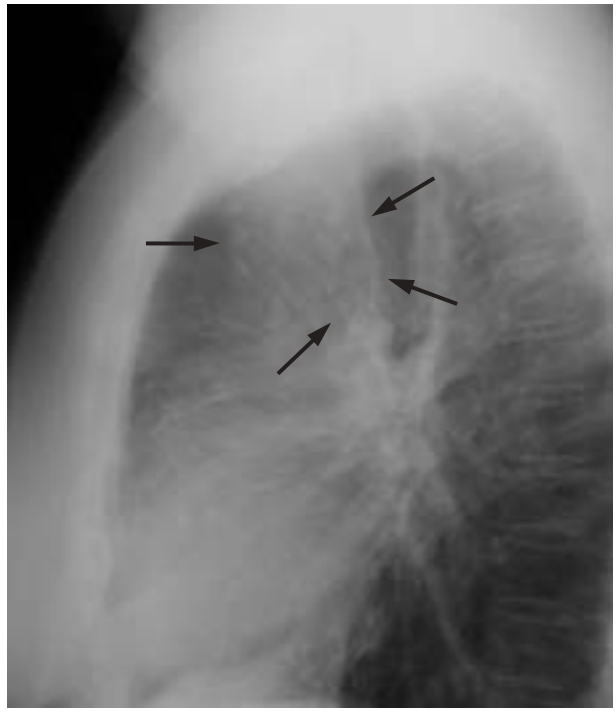

Fig. 3. – Lateral chest radiograph (detail) showing multiple calcified lymph nodes in the hilum and in the mediastinum (arrows). Most calcifications show an eggshell pattern (arrows).

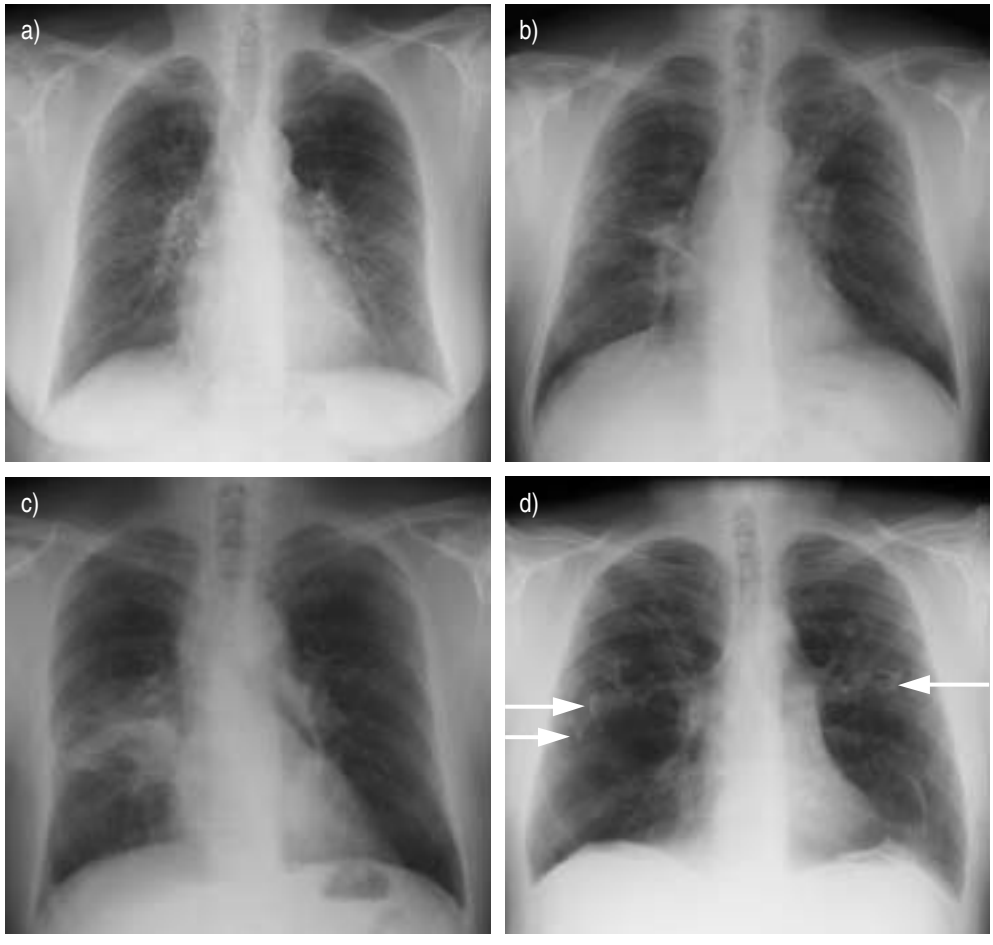

Fig. 4. – a) Reticular, b) reticulonodular and c) focal alveolar opacities are the most characteristic features on a chest radiograph. d) End-stage disease characterised by the presence of conglomerated masses and coarse septal bands with architectural distortion, hilar retraction and upper lobe volume loss. Notice also the pulmonary calcifications (arrows).

recognition of the axial distribution of the disease, whilst coronal reformations generated from spiral CT can more accurately show the craniocaudal distribution [25, 26]. Due to their higher density, resolution CT scans may detect parenchymal changes that are below the resolution of conventional chest radiographs. Moreover, with CT and, especially with HRCT, a detailed analysis of the lung parenchymal changes becomes possible and this technique can often depict whether a disease shows a predominant vascular, airway or lymphatic distribution or whether the disease is predominantly located in the interstitial tissue. This is particularly helpful in the diagnosis of sarcoidosis. Indeed, sarcoid granulomas are typically distributed along the lymphatic vessels, which run within the interstitial tissues of the bronchovascular bundles down to the terminal bronchioles, in the interlobular septa and subpleural [27].

The (HR)CT features of lung parenchymal involvement in sarcoidosis depend upon the stage and chronicity of the disease. Nodules which vary in size from 2 mm to 1 cm are the most commonly seen pulmonary parenchymal abnormality (fig. 5) [28–32]. These nodules represent aggregates of granulomas, with or without peribronchiolar fibrosis

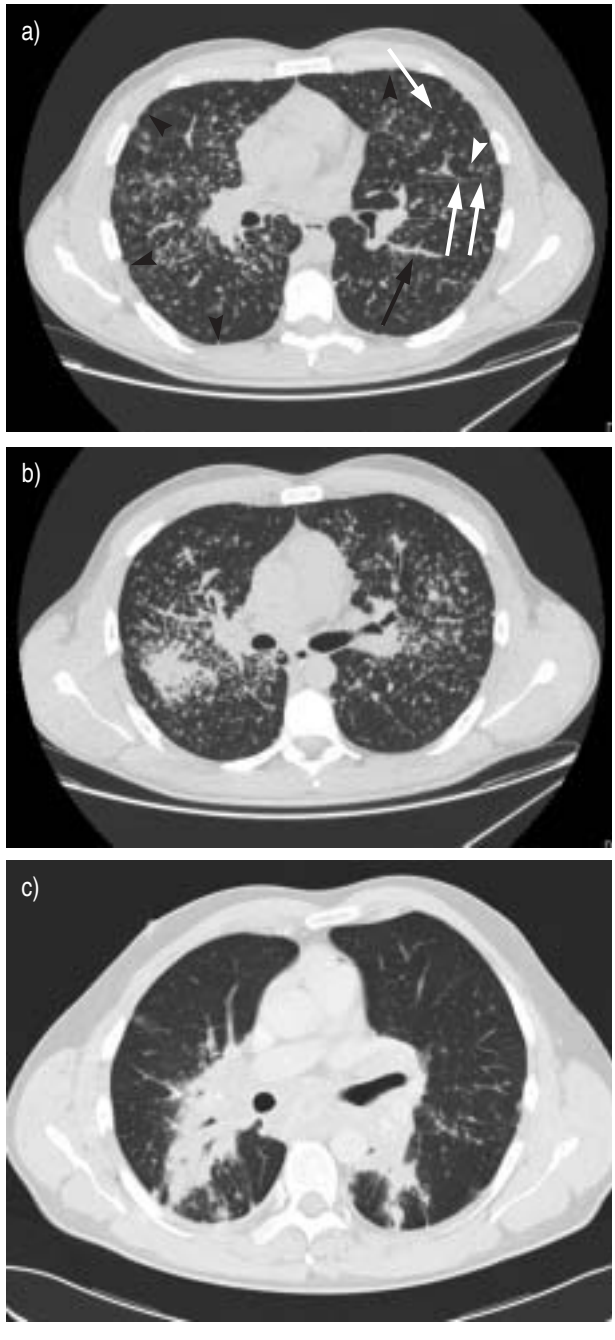

Fig. 5. – Nodules representing aggregates of granulomas are the most commonly seen pulmonary parenchymal abnormality on computed tomography (CT) (a–c). They are typically located in the lymphatics along the large and small bronchovascular bundles (causing thickened bronchovascular bundles; black arrow), and, to a lesser extent, in the subpleural lymphatics (causing nodular delineation of the pleura and of the fissure; black arrowheads), in the interlobular septal (giving rise to a beaded appearance of these septa; white arrows) and centrilobular lymphatics (giving rise to peripheral centrilobular nodules; white arrowheads) (a and b). Confluent nodular opacities can present on CT as areas of lung consolidation, possibly with an air bronchogram (c).

[33]. On (HR)CT these nodules usually are sharply defined, have irregular margins [34] and are typically located in the lymphatics along the large and small bronchovascular bundles (causing thickened bronchovascular bundles), and to a lesser extent in the subpleural lymphatics (causing nodular delineation of the pleura and of the fissure), in the interlobular septal (giving rise to a beaded appearance of these septa) and centrilobular lymphatics (giving rise to peripheral centrilobular nodules) (fig. 5a, b) [32, 34, 35].

The thickening of the bronchovascular bundles and beaded appearance of the interlobular septa and fissures may mimic lymphangitic carcinomatosis, especially when this thickening is more uniform and less nodular. Differential diagnosis between the two entities is usually possible by the upper lobe preponderance in sarcoidosis, and the more extensive and linear thickening of the interlobular septa in lymphangitic carcinomatosis [36]. In addition, lymphangitic carcinomatosis is frequently unilateral, whereas sarcoidosis is typically bilateral in nature. The differential diagnosis with other nodular diseases is based on the study of the distribution pattern and the delineation of the nodules [37, 38]. Although sharply defined, haematogeneous metastases usually show a random distribution. Also, miliary infection (tuberculosis, fungus) shows a random distribution and can be well- or ill-defined. Hypersensitivity pneumonitis, bronchiolitis and haemorrhage can also have a nodular appearance but these nodules are usually ill-defined and located in the centre part of the secondary pulmonary lobule. Nodules seen in organising pneumonia and Langerhans cell histiocytosis are usually well-defined and also show a centrilobular distribution.

Confluent nodular opacities can present on CT as areas of lung consolidation with air bronchograms (fig. 5c). This parenchymal consolidation is usually bilateral and symmetrical and shows an upper and midlung distribution. Also, areas of ground-glass opacity may be seen. When ground-glass opacity is seen on thick-slice CT scans, small nodules may be identified on thinner slices [39]. The cause of ground-glass attenuation on HRCT is uncertain. It has been suggested that this feature corresponds to active alveolitis and reversible disease (fig. 6a) [40]. However, ground-glass opacity with a coarse texture and with traction bronchiectasis may reflect irreversible fibrotic changes (fig. 6b). It should be emphasised, however, that these areas of ground-glass opacity can be caused by increased perfusion secondary to vascular redistribution. This vascular redistribution is secondary to the decreased perfusion in the surrounding areas which results from hypoventilation caused by bronchiolar narrowing (mosaic pattern) (fig. 6c and d). Sometimes a "crazy paving" pattern can be observed. This pattern consists of ground-glass attenuation with superimposed interlobular septal thickening [41].

Although lung nodules and consolidation, when evaluated over time, often disappear or decrease in number and extent, fibrosis may develop in advanced disease and signs that reflect irreversible disease can then be observed [42–44]. These signs include fibrous bands, and architectural distortion of the fissures, (thickened) interlobular septa, bronchi and blood vessels (fig. 7a). Also, retraction of the hila, bronchiectasis and cystic radiolucencies including cysts, bullae and paracicatricial emphysema, are seen (fig. 7b) [29, 31, 32]. These fibrotic and cystic changes are typically worse in the upper lobes and follow large airways in a perihilar distribution (fig. 7) [30, 34, 45, 46]. This upper lobe and perihilar distribution is usually specific enough to suggest the diagnosis of sarcoidosis, although in a very small percentage of patients sarcoidosis may produce HRCT signs almost identical to idiopathic pulmonary fibrosis, *i.e.* signs of fibrosis in a peripheral, subpleural and lower lobe distribution [47]. Mycetomas may complicate upper lobe bullae [34]. In some patients, dense mass-like lesions with air bronchograms may be observed [31, 33, 42, 44]. These correspond to bronchial and bronchiolar dilatation with surrounding fibrosis.

Air-trapping is another very common CT feature in patients with sarcoidosis and

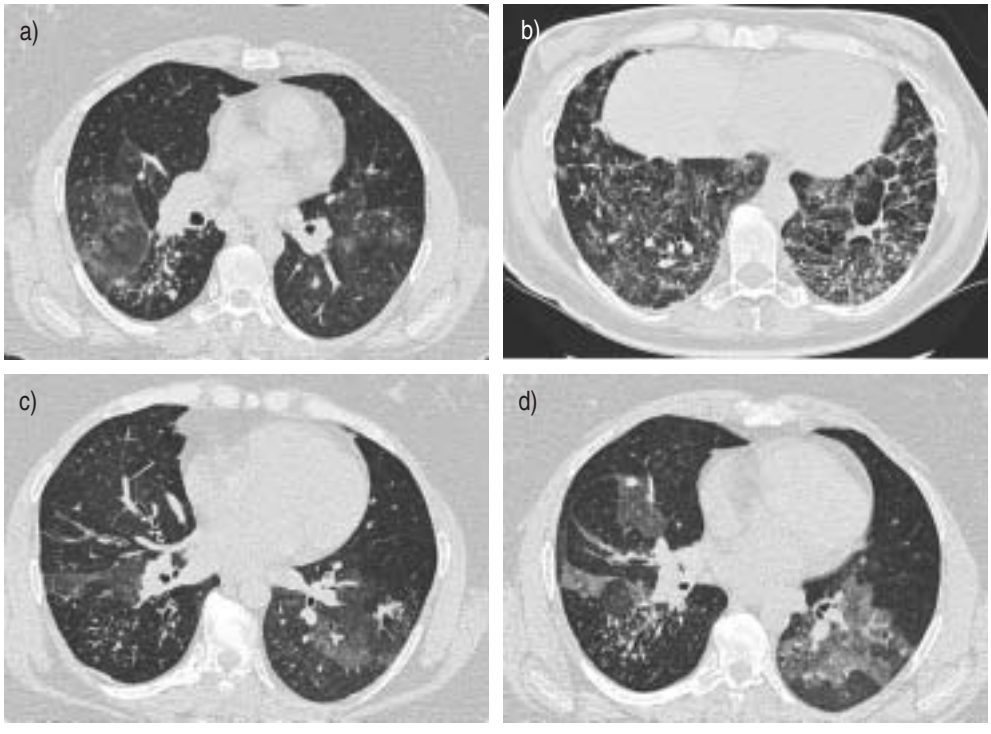

Fig. 6. – Ground-glass opacity on thin-slice computed tomography can indicate active a) alveolitis, but it can also be caused by b) irreversible fibrosis and by c) increased perfusion secondary to vascular redistribution (mosaic pattern). This mosaic pattern is accentuated on expiratory scans (d).

is seen in all stages of the disease [29, 48–50]. This sign can only be appreciated on expiratory CT scans and is characterised by the presence of multiple patchy areas of decreased attenuation, *i.e.* areas that do not increase in density and decrease in size on the expiratory scans (fig. 8). Often the lung attenuation is normal on inspiratory scans, although, as mentioned earlier, in some patients a mosaic pattern is already seen on the inspiratory scans (fig. 6c and d). Air-trapping is very common and was noted in 89% of patients in one study and in 95% of patients in another study [29, 49]. It may involve any

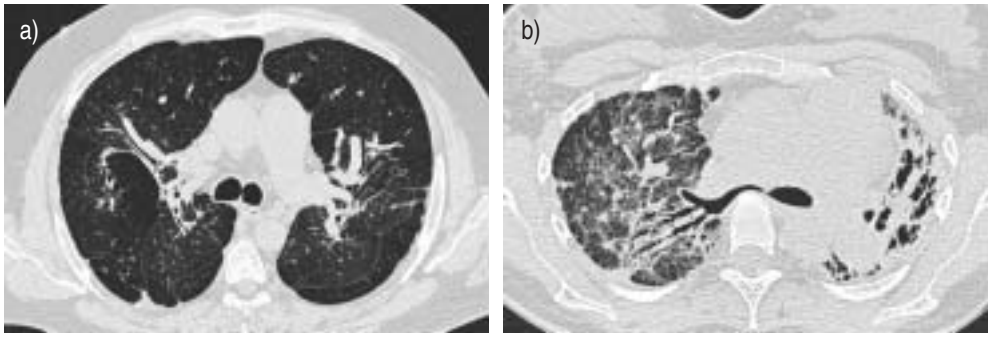

Fig. 7. – Advanced disease with lung fibrosis characterised by the presence of fibrous bands, architectural distortion of the fissures, septa, bronchi and blood vessels (a and b). Also retraction of the hila, bronchiectasis and cystic radiolucencies can be seen (b).

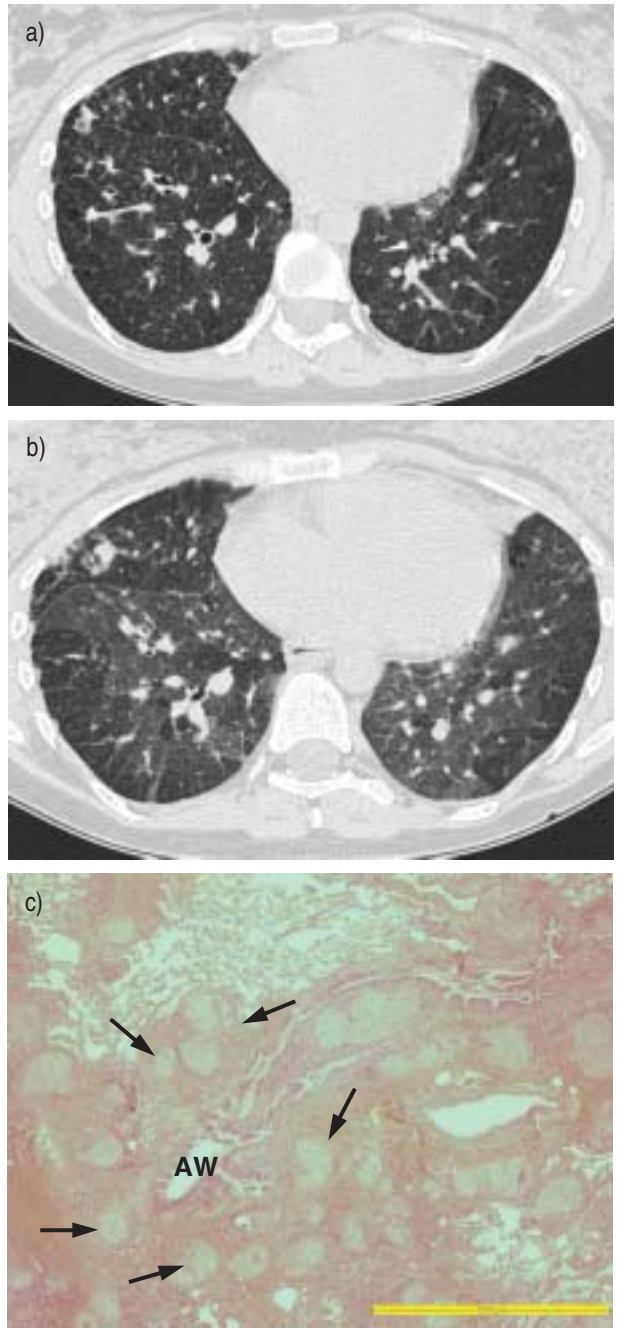

Fig. 8. – High-resolution computed tomography (HRCT) at a) end-inspiration and b) at end-expiration. c) Air-trapping is very common, may involve any lung zone and reflects small airway narrowing caused by granulomas (arrows) adjacent to the small airways (AW). Scale bar=1,000 μm. Figure 8c appears courtesy of B. Vrugt (Dept of Pathology, Martini Hospital, Groningen, The Netherlands).

lung zone and may be the only CT feature of pulmonary sarcoidosis [51]. It reflects small airway narrowing, which is very probably caused by granulomas adjacent to the small airways (fig. 8c) [52].

It should be emphasised that multiples of these CT patterns may co-exist in individual patients (the combination of central homogeneous areas of lung consolidation and surrounding small nodules is very suggestive for sarcoidosis) and may evolve over time, and that signs of potentially reversible disease can be seen in combination with findings that reflect irreversible fibrosis [53]. Table 1 shows the most frequent CT features of sarcoidosis.

Uncommon features

Although more frequently seen on a CT scan than on a chest radiograph, primary cavitation as a result of central necrosis due to confluent granulomas is rare. It was evident in <1% of patients on a chest radiograph in one study and in 2% of patients on CT in another study [54, 55]. If cavitation occurs, superimposed infection should be considered.

Pleural effusion is seen in only 1–4% of patients with sarcoidosis on a chest radiograph and a little more frequently on CT scans [21, 44, 56, 57]. Pleural thickening is often seen and is usually not caused by pleural involvement with sarcoidosis, but is the result of fibrotic retraction of extrathoracic soft tissue and fat.

As mentioned earlier fibrotic changes are often responsible for the development of small bullous changes (fig. 7b). More rarely, large bullae develop [58]. The cause of these lesions is unknown. Possible causes include air-trapping and alveolar distension due to bronchiolar narrowing, destruction of lung tissue by active alveolitis and retraction and collapse of the surrounding lung with air-filling of more compliant airspaces [59].

Rarely sarcoidosis presents as a solitary pulmonary nodule (fig. 9) [22, 60, 61].

Mycetomas may develop in any of the above mentioned cystic spaces and are seen in about 1–3% of patients [62, 63]. Typically they develop in the upper lobes [62, 64]. The observer should be alerted when new pleural thickening adjacent to a known cystic space develops because this can be the first sign of a developing mycetoma.

Pneumothorax is another rare manifestation of sarcoidosis which usually occurs late in the course of the disease [65].

Disease activity and correlation with pulmonary function

Although its value is relatively limited, the chest radiograph is still widely used to predict the severity of pulmonary involvement and to have an idea about the prognosis of

Table 1. – CT features of sarcoidosis

Sharply defined nodular opacities located in the central lung and upper lobes in:
The peribronchovascular interstitium
Relation to the centrilobular structures
The interlobular septa
The pleural surfaces
Large nodules, lung consolidation and conglomerate masses
Ground-glass opacity
Mosaic attenuation and air-trapping
Findings of fibrosis:
Septal thickening
Traction bronchiectasis
Honeycombing
Mediastinal and hilar lymph node enlargement, usually symmetrical

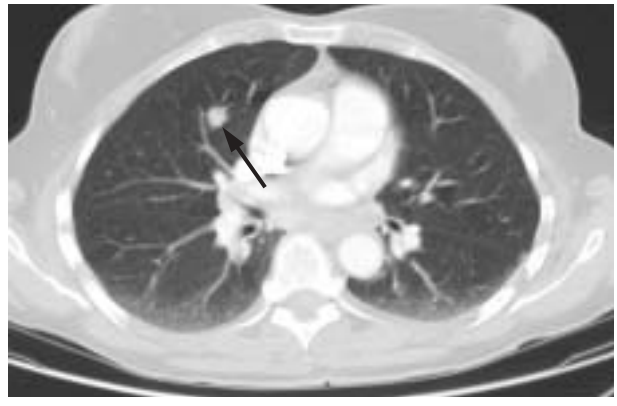

Fig. 9. – Sarcoidosis presenting as a solitary pulmonary nodule (arrow).

disease (table 2) [66, 67]. A score based on chest radiograph findings is used and defines five radiographic stages of intrathoracic changes, including: stage 0: normal chest radiograph; stage 1: lymphadenopathy only; stage 2: lymphadenopathy with parenchymal infiltration; stage 3: parenchymal disease only; stage 4: pulmonary fibrosis [1]. The limited value of this score is related to the complexity of the lung involvement with both airway and interstitial changes often not visible on a conventional chest radiograph and resulting in complex lung function abnormalities [68].

Given the better image quality and the higher density resolution of CT and HRCT, allowing an earlier detection of disease and a better study of its extent, it can be expected that this technique is more valuable in evaluating parameters of disease activity and functional impairment. Several investigators have indeed evaluated the type and extent of disease on CT and their correlations with pulmonary function. Various attempts were also made to score sarcoidosis with HRCT based on different criteria [28, 69–72].

MÜLLER *et al.* [30] compared findings of sarcoidosis on thick-slice CT scans (10 mm) and chest radiographs with dyspnoea scores and pulmonary function tests (PFTs) and found significant correlations. The extent of disease on CT correlated slightly better with the carbon monoxide diffusing capacity of the lung ($D_{L,CO}$) than did the profusion of opacities on chest radiographs, but correlations of CT with other PFT parameters, such as vital capacity (VC) and total lung capacity (TLC) were similar to chest radiographs; these authors suggested that neither CT nor the chest radiograph can be considered a good predictor of functional impairment in any individual patient with sarcoidosis. Similar observations were made by others [31, 71]. In contrast, BRAUNER *et al.* [31] found weak correlations between CT scores of sarcoidosis and different functional parameters, such as TLC, VC, forced expiratory volume in one second and $D_{L,CO}$ but these correlations were no better than conventional chest radiographs. Also REMY-JARDIN *et al.* [71] found a significant but weak correlation between the extent of abnormalities on CT and impairment of lung function. However, these lung changes did not reflect disease

Table 2. – Chest radiograph scoring of sarcoidosis[#]

Stage 0: 5–15
Stage 1: 45–65
Stage 2: 30–40
Stage 3: 10–15
Stage 4: 5

[#]: Table shows the percentages of patients in each stage at the time of presentation.

activity. Other studies looked at the patterns of CT abnormality and found that the pattern of CT abnormality influenced PFT results [29, 45, 69]. In one study, bronchial distortion was associated with lower expiratory flow rates, while the honeycomb pattern was more associated with restriction and reduced $D_{L,CO}$, TLC and forced vital capacity (FVC) [69]. DAVIES *et al.* [49] found that the extent of air-trapping correlated with percentage of predicted (% pred) residual volume/TLC and % pred maximal mid-expiratory flow rate between 25–75% of the VC. MAGKANAS *et al.* [51] found a significant correlation between the extent of air-trapping and the residual volume and the residual volume-total lung capacity ratio. Although these studies showed, among selected patient groups, modest to good correlations between some radiographic and CT features and some PFT parameters, the practical value of these associations in the individual patient is limited and it is doubtful whether it gives any benefit in the management of this patient [73].

Also the attempts to produce CT scoring systems for sarcoidosis were not always successful [28, 69–72]. OBERSTEIN *et al.* [74] described a HRCT scoring system which registers quality and quantity of lung parenchyma affected, pleural thickening and enlargement of lymph nodes; they found a good correlation between their scoring system and the number of polymorphous clear neutrophils in BAL fluid which was found to be related to disease severity [74–76]. DRENT *et al.* [68] used a HRCT scoring system adapted from OBERSTEIN *et al.* [74] containing six HRCT patterns: 1) thickening or irregularity of the bronchovascular bundle; 2) parenchymal consolidation, including ground-glass opacifications; 3) intraparenchymal nodules; 4) septal and nonseptal lines; 5) focal pleural thickening; and 6) enlargement of the lymph nodes. They found that the scores of thickening or irregularity of the bronchovascular bundle, intrapulmonary nodules, septal and nonseptal lines, and focal pleural thickening were significantly correlated with several pulmonary function parameters both at rest and at maximal exercise. Parenchymal consolidations, including ground-glass opacifications, and enlargement of lymph nodes turned out to be of minor importance.

Some CT features have prognostic significance, but because of the important variability between patients it is doubtful whether CT can predict disease outcome or response to therapy. Certain CT features, such as distortion, cysts, traction bronchiectasis and bronchiolectasis reflect fibrosis and indicate poor responsiveness to therapy [42–45, 71, 77]. In contrast, nodular opacities, lung consolidation, ground-glass opacity, and septal and nonseptal lines may represent either granulomatous inflammation or fibrosis or a combination of both changes and are potentially reversible with appropriate therapy [28, 41–43, 45, 71, 77]. Ground-glass opacity showed the same characteristics as in other diffuse lung diseases [78]; it may be a sign of acute inflammation and reversible disease but with a coarse texture and with traction bronchiectasis or bronchiolectasis it more likely reflects irreversible fibrotic changes. One study also showed that air-trapping was in part reversible under steroid treatment [79], confirming the observation that airway obstruction, as measured with PFTs, can be reversed by treatment [80].

Cardiac involvement

Although cardiac involvement is often present (it was observed in 25% of patients in an autopsy series [81]), it is only depicted in ~5% of patients [82]. Patients are very often asymptomatic, but when the conduction pathway is involved symptoms, such as ventricular arrhythmia and heart blockage, which may result in sudden cardiac arrest, can occur [83]. In fact, cardiac sarcoidosis is responsible for 50% of deaths [83, 84]. Also, congestive heart failure is sometimes seen.

CT is of little value in the diagnosis of cardiac sarcoidosis. Some myocardial thinning at the site of involvement is occasionally seen. MRI is a better technique and can be used for early detection of disease. The sites of involvement manifest as areas of increased signal intensity on T2-weighted images or as areas of enhancement on T1-weighted images (fig. 10) [85].

Extrathoracic involvement (selected sites)

Central nervous system involvement

Up to 25% of patients with sarcoidosis have asymptomatic involvement of the CNS at autopsy [86–88]. However, clinically recognisable disease is seen in <10% of patients [86, 87]. Neurosarcoidosis has a predilection for the base of the brain and can cause cranial nerve palsy as one of the first symptoms [89]. The optic nerve and chiasm are also frequently involved [90, 91]. Gadolinium-enhanced MRI is the imaging modality of choice because it is more sensitive than CT and can depict a wide spectrum of abnormalities (fig. 11) [92]. The lesions can be solitary or multiple and typically present as hyperintense masses on T2-weighted images [93]. After administration of contrast these lesions typically enhance when biologically active. Signal intensity decreases in response to therapy (fig. 11b). Unfortunately, MRI may be normal in much localised disease while infections, some malignancies, vasculitis and multiple sclerosis can produce MRI features similar to those seen in sarcoidosis [94]. Sarcoidosis can also cause aseptic meningitis. The meningeal lesions are usually not seen on unenhanced MRI but often show diffuse enhancement on contrast-enhanced (CE) T1-weighted imaging. Also, the spinal cord can be involved. On T2-weighted MRI, an intramedullary lesion with decreased signal intensity can be observed. These lesions show enhancement on contrast-enhanced T1-weighted images [93, 95].

Ocular involvement is seen in up to 80% of patients and typically presents as a bilateral uveitis [1]. Involvement of the lacrimal glands can also occur and is commonly bilateral. CE CT or MRI typically shows enlarged, enhancing lacrimal glands.

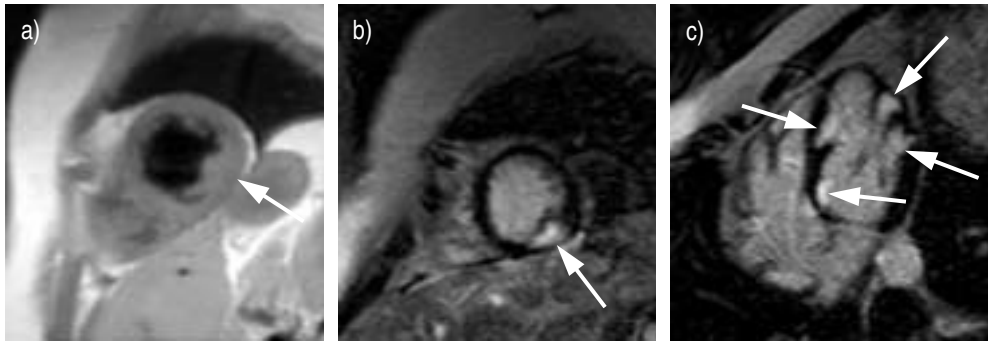

Fig. 10. – Cardiac sarcoidosis in a female aged 41 yrs presenting with asymptomatic atrioventricular block. a) T1-weighted fast spino-echo (SE) magnetic resonance imaging (MRI). b) Contrast-enhanced inversion recovery (CE-IR) MRI with late imaging in the cardiac short-axis (same level as a), and c) horizontal long-axis. Moderate thickening of the inferolateral LV wall is visible on SE-MRI (a; arrow). In this area, a focal strong enhancement is found with a thin nonenhancing subendocardial and subepicardial rim (b; arrow). On the horizontal long-axis view, several areas of strong enhancement are found throughout the LV wall, probably representing several noncaseating granulomas (c; arrows). Scans appear courtesy of J. Bogaert (Dept of Radiology, University Hospitals, Leuven, Belgium).

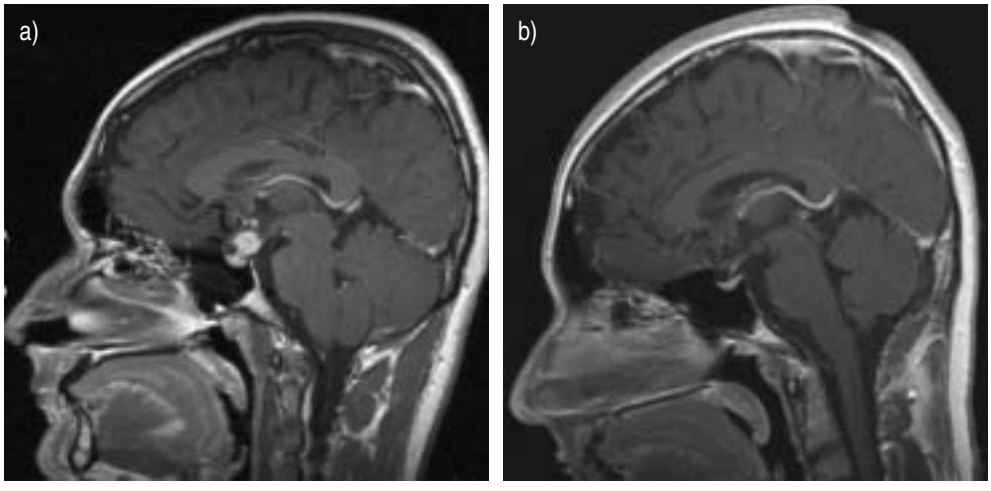

Fig. 11. – Neurosarcoidosis a) before and b) after treatment. Sagittal gadolinium-enhanced T1-weighted spin-echo image showing an infundibular mass in the pituitary stalk (a). After treatment (b), no residual mass is seen. Scans appear courtesy of P. Demaerel (Dept of Radiology, University Hospitals, Leuven, Belgium).

Abdominal involvement

As in the CNS, many patients with sarcoidosis show liver and spleen involvement at autopsy, but only few develop dysfunction of these organs [96]. Usually some enlargement of liver and spleen is seen and can be depicted with CT and MRI. Only 10–15% of patients show hypointense and hypoattenuating liver and/or spleen nodules ranging in size from 5–20 mm that correspond with coalescing granulomas [96–101]. Differential diagnosis with more common diseases, such as metastases and lymphoma can be difficult. In lymphoma, however, lymph node enlargement is more pronounced and the retrocrural lymph nodes are more frequently involved [96, 99]. Simultaneous involvement of liver and spleen makes metastatic disease less likely and favours the diagnosis of sarcoidosis and lymphoma.

Involvement of the gastrointestinal tract is rare and when present it is usually associated with pulmonary disease [102]. The stomach is the most common site of involvement and the radiological signs of the disease are very aspecific ranging from mucosal thickening, mimicking Menetrier disease, to lesions, mimicking gastric ulcers or linitis plastica.

Involvement of the genitourinary tract is seen in <5% of patients. Sarcoidosis most frequently affects the kidneys, but in male patients the epididimys and the testis can also be involved [103]. CE CT scan may show signs of interstitial nephritis or less frequently multiple low-attenuation nodules that resemble lymphoma or metastases [104, 105]. When the epididimys is involved, MRI can show heterogeneous and nodular enlargement with a slight increase in signal intensity on the T2-weighted image [103].

Other sites of involvement

Extrathoracic lymphadenopathy can be seen in sarcoidosis patients. Indeed, about one-third of patients indeed have enlarged cervical lymph nodes and their recognition is important in case a biopsy is considered. Massive abdominal lymphadenopathy, especially in the paraaortic region does also occur but is relatively rare. Imaging

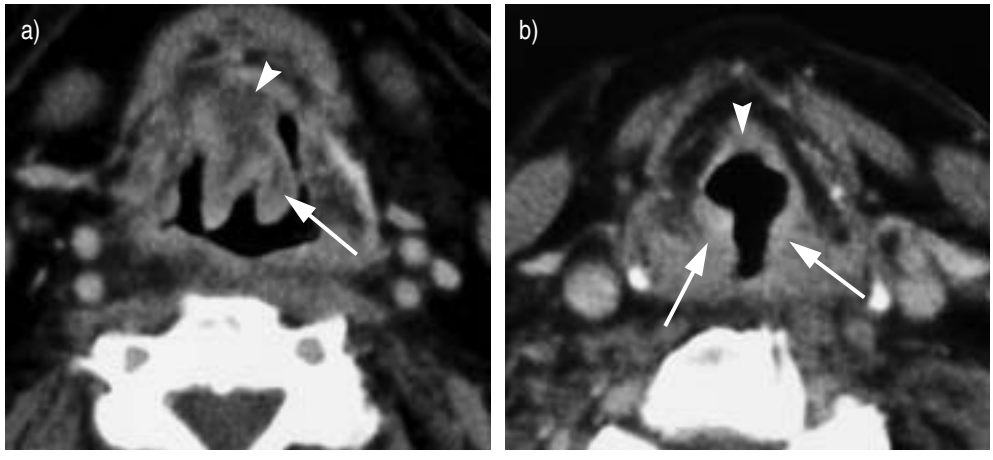

Fig. 12. – Sarcoidosis of the epiglottis. Axial contrast-enhanced computed tomography images. a) Thickening and superficial enhancement of the free edge of the epiglottis (arrow), with marked infiltration of the pre-epiglottic fat (arrowhead). b) Slightly thickened infrahyoid epiglottis (arrowhead); the aryepiglottic folds (arrows) also appear thickened and show superficial enhancement. Scans appear courtesy of R. Hermans (Dept of Radiology, University Hospitals, Leuven, Belgium).

appearances of these nodes are, however, aspecific and differentiation from metastatic disease or malignant lymphoma may be difficult.

Involvement of the parotic glands is seen in ~6% of patients with sarcoidosis and is commonly bilateral and associated with widespread disease in other organs [1, 106]. MRI shows enlarged parotid glands, demonstrating increased signal intensity on T2-weighted images and enhancement after administration of contrast. Also, involvement of the epiglottis is possible (fig. 12).

The musculoskeletal system can also be involved, but usually this only occurs when the disease is generalised. Inflammatory changes in the joints are usually not identified radiologically but can be identified with MRI. When the muscles in particular are involved, characteristic nodules may appear [107]. These nodules typically show low signal intensity in the central part, which is related to the fibrotic changes while, because of the presence of granulomas, the periphery of the nodules exhibits bright signal intensity on T2-weighted images and enhancement after administration of contrast [108]. Skeletal involvement is seen in ~5–10% of patients with sarcoidosis and the disease most frequently affects the phalanges of the hands and feet, although involvement of the vertebral bodies can occur [109, 110]. Radiographic signs include intact articular spaces, bone erosion, which can be extensive and result in pathological fractures, and multiple cyst-like radiolucent areas. Often a subcutaneous soft tissue mass is also present [111]. Long bone and axial skeletal involvement may, however, be occult at conventional radiography, but depicted at MRI, with an appearance that resembles that of osseous metastases [112].

Summary

The diagnosis of sarcoidosis is usually established on the basis of clinical and radiological findings supported by histological findings. More than 80% of patients with sarcoidosis have intrathoracic adenopathy at the time of presentation. When hilar adenopathy is present, this intrathoracic adenopathy is often easily recognised on a chest radiograph. Computed tomography (CT) can depict additional mediastinal lymph nodes that are hardly or not visible on a chest radiograph. However, CT, and especially high-resolution CT, is especially helpful when pulmonary parenchymal disease is present. While some CT signs are moderately characteristic for the disease, CT can also play a role in the study of disease extent and can, to a certain degree, predict the reversibility of lung changes. Although magnetic resonance imaging may be useful in the evaluation of mediastinal and pulmonary involvement, the main development of this technique has taken place in the evaluation of neurosarcoidosis, and to a lesser degree in bone, muscle and cardiac sarcoidosis.

Keywords: Computed tomography, imaging, interstitial lung disease, sarcoidosis.

References

1. Statement on sarcoidosis. Joint statement of the American Thoracic Society (ATS), the European Respiratory Society (ERS) and the World Association of Sarcoidosis and Other Granulomatous Disorders (WASOG) adopted by the ATS Board of Directors and by the ERS Executive Committee, February 1999. *Am J Respir Crit Care Med* 1999; 160: 736–755.
2. Newman LS, Rose CS, Maier LA. Sarcoidosis. *N Engl J Med* 1997; 336: 1224–1234.
3. Lynch J, Kazerooni E, Gay S. Pulmonary sarcoidosis. *Clin Chest Med* 1997; 18: 755–785.
4. Johns CJ, Michele TM. The clinical management of sarcoidosis: a 50-year experience at the Johns Hopkins Hospital. *Medicine (Baltimore)* 1999; 78: 65–111.
5. Mana J, Teirstein AS, Mendelson DS, Padilla ML, DePalo LR. Excessive thoracic computed tomographic scanning in sarcoidosis. *Thorax* 1995; 50: 1264–1266.
6. Mana J. Magnetic resonance imaging and nuclear imaging in sarcoidosis. *Curr Opin Pulm Med* 2002; 8: 457–463.
7. Miller BH, Rosado-de-Christenson ML, McAdams HP, Fishback NF. Thoracic sarcoidosis: radiologic-pathologic correlation. *Radiographics* 1995; 15: 421–437.
8. James DG, Neville E, Siltzbach LE, *et al.* A worldwide review of sarcoidosis. *Ann NY Acad Sci* 1976; 278: 321–334.
9. Koyama T, Ueda H, Togashi K, Umeoka S, Kataoka M, Nagai S. Radiologic manifestations of sarcoidosis in various organs. *Radiographics* 2004; 24: 87–104.
10. Theros EG. RPC of the month from the AFIP. *Radiology* 1969; 92: 1557–1561.
11. Bein ME, Putman CE, McLoud TC, *et al.* A reevaluation of intrathoracic lymphadenopathy in sarcoidosis. *AJR Am J Roentgenol* 1978; 131: 409–415.
12. Sider L, Horton ES Jr. Hilar and mediastinal adenopathy in sarcoidosis as detected by computed tomography. *J Thorac Imaging* 1990; 5: 77–80.
13. Rockoff SD, Rohatgi PK. Unusual manifestations of thoracic sarcoidosis. *AJR Am J Roentgenol* 1985; 144: 513–528.
14. Hamper UM, Fishman EK, Khouri NF, *et al.* Typical and atypical CT manifestations of pulmonary sarcoidosis. *J Comput Assist Tomogr* 1986; 10: 928–936.

15. Gawne-Cain ML, Hansell DM. The pattern and distribution of calcified mediastinal lymph nodes in sarcoidosis and tuberculosis: a CT study. *Clin Radiol* 1996; 51: 263–267.
16. McLoud TC, Putman CE, Pascual R. Eggshell calcification with systemic sarcoidosis. *Chest* 1974; 66: 515–517.
17. Niimi H, Kang EY, Kwong JS, Carignan S, Muller NL. CT of chronic infiltrative lung disease: prevalence of mediastinal lymphadenopathy. *J Comput Assist Tomogr* 1996; 20: 305–308.
18. Bergin CJ, Coblentz CL, Chiles C, *et al.* Chronic lung diseases: specific diagnosis by using CT. *AJR Am J Roentgenol* 1989; 152: 1183–1188.
19. Wells A. Clinical usefulness of high resolution computed tomography in cryptogenic fibrosing alveolitis. *Thorax* 1998; 53: 1080–1087.
20. Battesti JP, Saumon G, Valeyre D, *et al.* Pulmonary sarcoidosis with an alveolar radiographic pattern. *Thorax* 1982; 37: 448–452.
21. Littner MR, Schachter EN, Putman CE, *et al.* The clinical assessment of roentgenographically atypical pulmonary sarcoidosis. *Am J Med* 1977; 62: 361–368.
22. Rose RM, Lee RG, Costello P. Solitary nodular sarcoidosis. *Clin Radiol* 1985; 36: 589–595.
23. Sharma OP, Hewlett R, Gordonson J. Nodular sarcoidosis: an unusual radiographic appearance. *Chest* 1973; 64: 189–192.
24. Tazi A, Desfemmes-Baleyte T, Soler P, *et al.* Pulmonary sarcoidosis with a diffuse ground-glass pattern on the chest radiograph. *Thorax* 1994; 49: 793–797.
25. Johkoh T, Muller NL, Nakamura H. Multidetector spiral high-resolution computed tomography of the lungs: distribution of findings on coronal image reconstructions. *J Thorac Imaging* 2002; 17: 291–305.
26. Eibel R, Turk T, Kulinna C, Schopf UJ, Bruning R, Reiser MF. Value of multiplanar reformations (MPR) in multi-slice spiral CT of the lung. *Röfo* 2001; 173: 57–64.
27. Kitaichi M. Pathology of pulmonary sarcoidosis. *Clin Dermatol* 1986; 4: 108–115.
28. Leung AN, Brauner MW, Caillat-Vigneron N, *et al.* Sarcoidosis activity: correlation of HRCT findings with those of 67Ga scanning, bronchoalveolar lavage, and serum angiotensin-converting enzyme assay. *J Comput Assist Tomogr* 1998; 22: 229–234.
29. Hansell DM, Milne DG, Wilsher ML, *et al.* Pulmonary sarcoidosis: morphologic associations of airflow obstruction at thin-section CT. *Radiology* 1998; 209: 697–704.
30. Müller NL, Mawson JB, Mathieson JR, *et al.* Sarcoidosis: correlation of extent of disease at CT with clinical, functional, and radiographic findings. *Radiology* 1989; 171: 613–618.
31. Brauner MW, Grenier P, Mompoint D, Lenoir S, deCremoux H. Pulmonary sarcoidosis: evaluation with high-resolution CT. *Radiology* 1989; 172: 467–471.
32. Muller NL, Kullnig P, Miller RR. The CT findings of pulmonary sarcoidosis: analysis of 25 patients. *AJR Am J Roentgenol* 1989; 152: 1179–1182.
33. Nishimura K, Itoh H, Kitaichi M, *et al.* Pulmonary sarcoidosis: correlation of CT and histopathologic findings. *Radiology* 1993; 189: 105–109.
34. Traill ZC, Maskell GF, Gleeson FV. High-resolution CT findings of pulmonary sarcoidosis. *AJR Am J Roentgenol* 1997; 168: 1557–1560.
35. Hwang JH, Kim TS, Lee KS, *et al.* Bronchiolitis in adults: pathology and imaging. *J Comput Assist Tomogr* 1997; 21: 913–919.
36. Honda O, Johkoh T, Ichikado K, *et al.* Comparison of high resolution CT findings of sarcoidosis, lymphoma, and lymphangitic carcinoma: is there any difference of involved interstitium? *J Comput Assist Tomogr* 1999; 23: 374–379.
37. Voloudaki AE, Tritou IN, Magkanas EG, Chalkiadakis GE, Siafakas NM, Gourtsoyiannis NC. HRCT in military lung disease. *Acta Radiol* 1999; 40: 451–456.
38. Gruden JF, Webb WR, Naidich DP, McGuinness G. Multinodular disease: anatomic localization at thin-section CT – multireader evaluation of a simple algorithm. *Radiology* 1999; 210: 711–720.
39. Müller NL, Miller RR. Ground-glass attenuation, nodules, alveolitis, and sarcoid granulomas. *Radiology* 1993; 189: 31–32.

40. Chiles C. Imaging features of thoracic sarcoidosis. *Semin Roentgenol* 2002; 37: 82–93.
41. Rossi SE, Erasmus JJ, Volpacchio M, Franquet T, Castiglioni T, McAdams HP. "Crazy-paving" pattern at thin-section CT of the lungs: radiologic-pathologic overview. *Radiographics* 2003; 23: 1509–1519.
42. Brauner MW, Lenoir S, Grenier P, *et al.* Pulmonary sarcoidosis: CT assessment of lesion reversibility. *Radiology* 1992; 182: 349–354.
43. Murdoch J, Müller NL. Pulmonary sarcoidosis: changes on follow-up CT examination. *AJR Am J Roentgenol* 1992; 159: 473–477.
44. Wells A. High resolution computed tomography in sarcoidosis: a clinical perspective. *Sarcoidosis Vasc Diffuse Lung Dis* 1998; 15: 140–146.
45. Abehsera M, Valeyre D, Grenier P, *et al.* Sarcoidosis with pulmonary fibrosis: CT patterns and correlation with pulmonary function. *AJR Am J Roentgenol* 2000; 174: 1751–1757.
46. Lynch J, Kazerooni E. Sarcoidosis. *In:* Sperber M, ed. Radiological Diagnosis of Chest Disease, 2nd Edn. London, Springer-Verlag, 2001; pp. 193–220.
47. Padley SP, Padhani AR, Nicholson A, Hansell DM. Pulmonary sarcoidosis mimicking cryptogenic fibrosing alveolitis on CT. *Clin Radiol* 1996; 51: 807–810.
48. Gleeson FV, Traill ZC, Hansell DM. Evidence of expiratory CT scans of small-airway obstruction in sarcoidosis. *AJR Am J Roentgenol* 1996; 166: 1052–1054.
49. Davies CW, Tasker AD, Padley SP, *et al.* Air trapping in sarcoidosis on computed tomography: correlation with lung function. *Clin Radiol* 2000; 55: 217–221.
50. Bartz RR, Stern EJ. Airways obstruction in patients with sarcoidosis: expiratory CT scan findings. *J Thorac Imaging* 2000; 15: 285–289.
51. Magkanas E, Voloudaki A, Bouros D, *et al.* Pulmonary sarcoidosis. Correlation of expiratory high-resolution CT findings with inspiratory patterns and pulmonary function tests. *Acta Radiol* 2001; 42: 494–501.
52. Shaw RJ, Djukanovic R, Tashkin DP, Millar AB, duBois RM, Orr PA. The role of small airways in lung disease. *Respir Med* 2002; 96: 67–80.
53. Johkoh T, Ikezoe J, Kohno N, *et al.* Usefulness of high-resolution CT for differential diagnosis of multi-focal pulmonary consolidation. *Radiat Med* 1996; 14: 139–146.
54. Mayock R, Bertrand P, Morrison C, *et al.* Manifestations of sarcoidosis: analysis of 145 patients, with a review of nine series selected from the literature. *Am J Med* 1963; 36: 67–89.
55. Grenier P, Brauner M, Valeyre D. Computed tomography in the assessment of diffuse lung disease. *Sarcoidosis Vasc Difffuse Lung Dis* 1999; 16: 47–56.
56. Soskel N, Sharma OP. Pleural involvement in sarcoidosis: case presentation and detailed review of the literature. *Semin Respir Med* 1992; 13: 492–514.
57. Sharma OP, Gordonson J. Pleural effusion in sarcoidosis: a report of six cases. *Thorax* 1975; 30: 95–101.
58. Packe GE, Ayres JG, Citron KM, *et al.* Large lung bullae in sarcoidosis. *Thorax* 1986; 41: 792–797.
59. Judson MA, Strange C. Bullous sarcoidosis: a report of three cases. *Chest* 1998; 114: 1474–1478.
60. Chrisholm JC, Lang GR. Solitary circumscribed pulmonary nodule: an unusual manifestation of sarcoidosis. *Arch Intern Med* 1966; 118: 376–378.
61. Pinsker KL. Solitary pulmonary nodule in sarcoidosis. *JAMA* 1978; 240: 1379–1380.
62. Tomlinson JR, Sahn SA. Aspergilloma in sarcoid and tuberculosis. *Chest* 1987; 92: 505–508.
63. Kaplan J, Johns CJ. Mycetomas in pulmonary sarcoidosis: nonsurgical management. *Johns Hopkins Med J* 1979; 145: 157–161.
64. Israel HL, Lenchner GS, Atkinson GW. Sarcoidosis and aspergilloma: the role of surgery. *Chest* 1982; 82: 430–432.
65. Froudarakis ME, Bouros D, Voloudaki A, *et al.* Pneumothorax as a first manifestation of sarcoidosis. *Chest* 1997; 112: 278–280.
66. Hunninghake GW, Costabel U, Ando M, *et al.* American Thoracic Society/European Respiratory Society/World Association of Sarcoidosis and other Granulomatous Disorders: statement on sarcoidosis. *Sarcoidosis Vasc Diffuse Lung Dis* 1999; 16: 149–173.

67. DeRemee RA. The roentgenographic staging of sarcoidosis: historic and contemporary perspectives. *Chest* 1983; 83: 128–133.
68. Drent M, DeVries J, Lenters M, *et al.* Sarcoidosis: assessment of disease severity using HRCT. *Eur Radiol* 2003; 13: 2462–2471.
69. Bergin CJ, Bell DY, Coblentz CL, *et al.* Sarcoidosis: correlation of pulmonary parenchymal pattern at CT with results of pulmonary function tests. *Radiology* 1989; 171: 619–624.
70. Mimori Y. Sarcoidosis: correlation of HRCT findings with results of pulmonary function tests and serum angiotensin-converting enzyme assay. *Kurume Med J* 1998; 45: 247–256.
71. Remy-Jardin M, Giraud F, Remy J, Wattinne L, Wallaert B, Duhamel A. Pulmonary sarcoidosis: role of CT in the evaluation of disease activity and functional impairment and in prognosis assessment. *Radiology* 1994; 191: 675–680.
72. Lynch DA, Webb WR, Gamsu G, Stulbarg M, Golden J. Computed tomography in pulmonary sarcoidosis. *J Comput Assist Tomogr* 1989; 13: 405–410.
73. Lynch JP 3rd. Computed tomographic scanning in sarcoidosis. *Semin Respir Crit Care Med* 2003; 24: 393–418.
74. Oberstein A, vonZitzewitz H, Schweden F, Müller-Quernheim J. Non-invasive evaluation of the inflammatory activity in sarcoidosis with high-resolution computed tomography. *Sarcoidosis Vasc Diffuse Lung Dis* 1997; 14: 65–72.
75. Drent M, Jacobs JA, DeVries J, Lamers RJS, Liem IH, Wouters EFM. Does the cellular bronchoalveolar lavage fluid profile reflect the severity of sarcoidosis? *Eur Respir J* 1999; 13: 1338–1344.
76. Ziegenhagen MW, Rothe ME, Schlaak M, Müller-Quernheim J. Bronchoalveolar and serological parameters reflecting the severity of sarcoidosis. *Eur Respir J* 2003; 21: 407–413.
77. Nishimura K, Itoh H, Kitaichi M, *et al.* CT and pathological correlation of pulmonary sarcoidosis. *Semin Ultrasound CT MR* 1995; 16: 361–370.
78. Remy-Jardin M, Giraud F, Remy J, *et al.* Importance of ground-glass attenuation in chronic diffuse infiltrative lung disease: pathologic-CT correlation. *Radiology* 1993; 189: 693–698.
79. Fazzi P, Sbragia P, Solfanelli S, Troilo S, Giuntini C. Functional significance of the decreased attenuation sign on expiratory CT in pulmonary sarcoidosis: report of four cases. *Chest* 2001; 119: 1270–1274.
80. Lavergne F, Clerici C, Sadoun D, Brauner M, Battesti JP, Valeyre D. Airway obstruction in bronchial sarcoidosis: outcome with treatment. *Chest* 1999; 116: 1194–1999.
81. Ratner SJ, Fenoglio JJ Jr, Ursell PC. Utility of endomyocardial biopsy in the diagnosis of cardiac sarcoidosis. *Chest* 1986; 90: 528–533.
82. Iwai K, Sekiguti M, Hosoda Y, *et al.* Racial difference in cardiac sarcoidosis incidence observed at autopsy. *Sarcoidosis* 1994; 11: 26–31.
83. Syed J, Myers R. Sarcoid heart disease. *Can J Cardiol* 2004; 20: 89–93.
84. Paule P, Braem L, Heno P, *et al.* Diagnosis of cardiac sarcoidosis and follow-up of 24 consecutive patients. *Rev Med Interne* 2004; 25: 357–362.
85. Vignaux O, Dhote R, Duboc D, *et al.* Clinical significance of myocardial magnetic resonance abnormalities in patients with sarcoidosis: a 1-year follow-up study. *Chest* 2002; 122: 1895–1901.
86. Manz HJ. Pathobiology of neurosarcoidosis and clinicopathologic correlation. *Can J Neurol Sci* 1983; 10: 50–55.
87. Chapelon C, Ziza JM, Piette JC, *et al.* Neurosarcoidosis: signs, course and treatment in 35 confirmed cases. *Medicine (Baltimore)* 1990; 69: 261–276.
88. Lury KM, Smith JK, Matheus MG, Castillo M. Neurosarcoidosis – review of imaging findings. *Semin Roentgenol* 2004; 39: 495–504.
89. Sharma OP. Neurosarcoidosis: a personal perspective based on the study of 37 patients. *Chest* 1997; 112: 220–228.
90. Zajicek JP, Scolding NJ, Foster O, *et al.* Central nervous system sarcoidosis: diagnosis and management. *Q J Med* 1999; 92: 103–117.

91. Smith JK, Matheus MG, Castillo M. Imaging manifestations of neurosarcoidosis. *Am J Roentgenol* 2004; 182: 289–295.
92. Sherman JL, Stern BJ. Sarcoidosis of the CNS: comparison of unenhanced and enhanced MR images. *AJNR Am J Neuroradiol* 1990; 11: 915–923.
93. Lexa FJ, Grossman RI. MR of sarcoidosis in the head and spine: spectrum of manifestations and radiographic response to steroid therapy. *Am J Neuroradiol* 1994; 15: 973–982.
94. Williams DW 3rd, Elster AD, Kramer SI. Neurosarcoidosis: gadolinium-enhanced MR imaging. *J Comput Assist Tomogr* 1990; 14: 704–707.
95. Fels C, Riegel A, Javaheripour-Otto K, Obenauer S. Neurosarcoidosis: findings in MRI. *Clin Imaging* 2004; 28: 166–169.
96. Warshauer DM, Molina PL, Hamman SM, *et al.* Nodular sarcoidosis of the liver and spleen: analysis of 32 cases. *Radiology* 1995; 195: 757–762.
97. Warshauer DM, Semelka RC, Ascher SM. Nodular sarcoidosis of the liver and spleen: appearance on MR images. *J Magn Reson Imaging* 1994; 4: 553–557.
98. Kessler A, Mitchell DG, Israel HL, *et al.* Hepatic and splenic sarcoidosis: ultrasound and MR imaging. *Abdom Imaging* 1993; 18: 159–163.
99. Britt AR, Francis IR, Glazer GM, *et al.* Sarcoidosis: abdominal manifestations at CT. *Radiology* 1991; 178: 91–94.
100. Warshauer DM, Dumbleton SA, Molina PL, *et al.* Abdominal CT findings in sarcoidosis: radiologic and clinical correlation. *Radiology* 1994; 192: 93–98.
101. Thanos L, Zormpala A, Brountzos E, Nikita A, Kelekis D. Nodular hepatic and splenic sarcoidosis in a patient with normal chest radiograph. *Eur J Radiol* 2002; 41: 10–11.
102. Farman J, Ramirez G, Rybak B, Lebwohl O, Semrad C, Rotterdam H. Gastric sarcoidosis. *Abdom Imaging* 1997; 22: 248–252.
103. Kodama K, Hasegawa T, Egawa M, Tomosugi N, Mukai A, Namiki M. Bilateral epididymal sarcoidosis presenting without radiographic evidence of intrathoracic lesion: review of sarcoidosis involving the male reproductive tract. *Int J Urol* 2004; 11: 345–348.
104. Sato A. Renal dysfunction in patients with sarcoidosis. *Intern Med* 1996; 35: 523–524.
105. Hughes JJ, Wilder WM. Computed tomography of renal sarcoidosis. *J Comput Assist Tomogr* 1988; 12: 1057–1058.
106. James DG, Sharma OP. Parotid gland sarcoidosis. *Sarcoidosis Vasc Diffuse Lung Dis* 2000; 17: 27–32.
107. Abril A, Cohen MD. Rheumatologic manifestations of sarcoidosis. *Curr Opin Rheumatol* 2004; 16: 51–55.
108. Otake S, Ishigaki T. Muscular sarcoidosis. *Semin Musculoskelet Radiol* 2001; 5: 167–170.
109. Mangino D, Stover DE. Sarcoidosis presenting as metastatic bony disease. A case report and review of the literature on vertebral body sarcoidosis. *Respiration* 2004; 71: 292–294.
110. Lisle D, Mitchell K, Crouch M, Windsor M. Sarcoidosis of the thoracic and lumbar spine: imaging findings with an emphasis on magnetic resonance imaging. *Australas Radiol* 2004; 48: 404–407.
111. Neville E, Carstairs LS, James DG. Sarcoidosis of bone. *Q J Med* 1977; 46: 215–227.
112. Moore SL, Teirstein AE. Musculoskeletal sarcoidosis: spectrum of appearances at MR imaging. *Radiographics* 2003; 23: 1389–1399.